

From CdS aggregate spheres to PbS hollow spheres: a case study of the growth mechanism in chemical conversion

Ning Liu · Dapeng Wu · Yi Jiang · Ying Xiao ·
Yafei Yuan · Kai Jiang

Received: 19 October 2010/Accepted: 24 December 2010/Published online: 11 January 2011
© Springer Science+Business Media, LLC 2011

Abstract Monodisperse PbS hollow spheres were successfully prepared via using CdS aggregate spheres as template. The present strategy is based on the different solubilities of CdS and PbS. This process was intensively studied by time-dependent trails which were monitored by transmission electron microscopy (TEM), field emission scanning electron microscopy (FESEM), X-ray diffraction (XRD), and photoluminescence spectroscopy (PL). Reaction temperature was found to play an important role in controlling the diffusion rate of Pb²⁺ ions and the quality of as-prepared PbS crystals, which finally leads to different shape evolution processes from the starting aggregate spheres to the final hollow spheres. Two growth mechanisms defined as kinetics-controlled process (KCP) and thermodynamics-controlled process (TDCP) were, respectively, proposed for the two conversion patterns observed at 30 and 90 °C. Moreover, specific structural evolution including primary crystal size, diameter growth, and shell thickness were also discussed in detail. This work is of great significance in elucidating the underlying mechanism of chemical conversion and could be potentially applied to synthesize other hollow architectures.

Introduction

Hollow-structured inorganic materials have recently attracted many research interests due to their promising applications in the fields such as solar cells, drug delivery, medical imaging, catalyst, and optical devices [1–9].

Chemical conversion is one of the most effective methods to fabricate materials with hollow structure. Generally, a layer of target product was firstly formed around the template by taking advantage of the different solubilities between the two materials. Afterwards, a suitable core removing reagent was adopted to dissolve the inner template leaving intact hollow shell. Heretofore, various hollow structures, such as ZnS, Ag₂S, and CuS, have been synthesized through this strategy [10–16]. However, the core removing reagents usually pose negative impacts on the crystal quality and integrity of the final hollow structures. Therefore, in order to fabricate intact hollow architectures, one step conversion, which avoids using the core removing regents, is of crucial importance. Furthermore, the one-pot synthesis is more cost efficient, time saving and easy for scale up. However, this method was seldom reported previously [17, 18].

Lead sulfide (PbS) is a well-known II–VI group semiconductor with narrow bulk band gap (0.41 eV at 300 K) and a relatively large excitation Bohr radius (18 nm), which contributes to the strong quantum confinement effect over a large nanocrystalline size range [17]. Therefore, PbS could be applied in various territories, such as photovoltaic cells, IR photodetectors, thermal and biological images, and display devices [19–25]. Due to the structural advantages, PbS hollow structures exhibit enhanced properties compared with bulk materials. Therefore, many efforts have been devoted to prepare different PbS hollow structures. However, these reported methods always require tedious procedures and rigid conditions [26, 27]. In this paper, we successfully prepared PbS hollow spheres by a facial chemical conversion process using CdS aggregate spheres as template. It is interesting to find the conversion takes two different ways in transforming the CdS aggregate spheres into PbS hollow spheres when the reaction is

N. Liu · D. Wu · Y. Jiang · Y. Xiao · Y. Yuan · K. Jiang (✉)
Chemistry and Environmental College, Henan Normal University, Xinxiang 453007, China
e-mail: jiangkai6898@126.com

carried out at different temperatures. These two processes were, respectively, studied by time-dependent trials and monitored by TEM and XRD. When the temperature is 30 °C, a gentle conversion defined as kinetics-controlled process (KCP) was observed, in which the CdS core dissolved gradually along with an inward growth of the PbS shell. On the other hand, when the temperature is elevated to 90 °C, the conversion takes a radical way defined as thermodynamics-controlled process (TDCP) [28]. In the later process, the CdS sphere was firstly converted into solid PbS sphere before it was transformed into hollow sphere via Oswald ripening [29]. This study may shed some lights on the mechanism of chemical conversion which received more and more attentions in fabricating hollow structures. Moreover, the photoluminescence properties of these products were also investigated under room temperature.

Experimental

Chemical

All reagents are of analytical grade and used as received without further purification. $\text{Cd}(\text{NO}_3)_2 \cdot 4\text{H}_2\text{O}$ and $\text{Pb}(\text{NO}_3)_2$ were obtained from Beijing Chemical Co., Ltd, Thiourea was purchased from Tianjin Bodi Chemical Co., Ltd and the poly(vinylpyrrolidone) (PVP) (K-30 MW = 10,000) was obtained from Tianjin Guangfu fine chemical research institution. Double-distilled water was used throughout the synthesis procedure.

Preparation of CdS aggregate spheres

The synthesis of CdS aggregate spheres was described elsewhere and received a slight modification [30]. 2.59 g of $\text{Cd}(\text{NO}_3)_2 \cdot 4\text{H}_2\text{O}$ was firstly dissolved into 84 mL ethylene glycol. Then 0.63 g of thiourea and 0.93 g PVP were added into the above solution under rigid stirring. Subsequently, the mixture was transferred to 120 mL Teflon-lined autoclave and heated at 140 °C for 8 h. The yellow products were centrifuged, washed with double-distilled water and absolute ethanol several times and finally dried at 60 °C for 5 h.

Preparation of PbS hollow spheres

100 mg CdS templates were homogeneously dispersed in 80 mL 0.3 M $\text{Pb}(\text{NO}_3)_2$ solution by ultrasonic irradiation. The suspension was kept in 30 °C water bath for 14 h with magnetic stirring. The black precipitate was centrifuged, washed with distilled water and ethanol several times, and finally dried in vacuum at 60 °C for 5 h to yield uniform PbS hollow spheres (marked as sample 1).

In the other synthesis, the reaction was carried out in 90 °C water bath while keeping other parameters unchanged. After reacted for 2 h, the black product was centrifuged, washed with distilled water and ethanol several times, and finally dried in vacuum at 60 °C for 5 h (marked as sample 2).

In order to investigate the growth mechanism, intermediate samples were collected at different time intervals during these two processes.

Characterization

The morphology and structure of the samples were characterized using field emission scanning electron microscopy (FESEM, JEOL 7041F) and transmission electron microscopy (TEM, JEOL JEM-100SX). X-ray diffraction (XRD) was carried out using Bruker advance-D8 XRD with Cu K α radiation ($\lambda = 0.154178$ nm). The accelerating voltage was set at 40 kV with a 100 mA flux. The UV-vis absorption spectra were obtained on model T6 UV-vis spectrophotometer which is manufactured by Beijing Purkinje General Instrument Co., Ltd, China. Photoluminescence (PL) spectra were measured at room temperature on JASCO FP-6500 fluorophotometer.

Results and discussion

XRD patterns of the CdS template, sample 1 and sample 2 are depicted in Fig. 1. All the diffraction peaks of CdS template can be indexed to (100), (002), (101), (110), (103), and (112) planes, which match well with the wurtzite structure CdS (JCPDS Card. 01-0780). The average size of the CdS spheres is calculated to be about 8 nm based on Scherrer's equation, which implies these spheres are aggregated from small primary crystals. The PbS hollow spheres prepared in this work all have cubic rock-salt structure (JCPDS Card. 65-2935). The diffraction peaks are sharp and no impurity peak is detected, which indicates the high quality and purity of as-prepared products. Compared with sample 1, the diffraction peaks of sample 2 are strong and sharp suggesting the sample prepared under high temperature possesses better crystal quality. Moreover, the peak width of sample 2 is narrower than that of sample 1 implying the primary particle composed in sample 2 has greater diameter. This size growth of the primary particles will be further discussed in detail later in this paper.

Figure 2 displays the FESEM and TEM images of the CdS spheres and the PbS hollow spheres prepared under different temperatures. Figure 2a and b show the as-formed CdS spheres are uniform in diameter and the average diameter is measured to be about 280 nm (calculated from 100 particles from the FESEM image). From the TEM

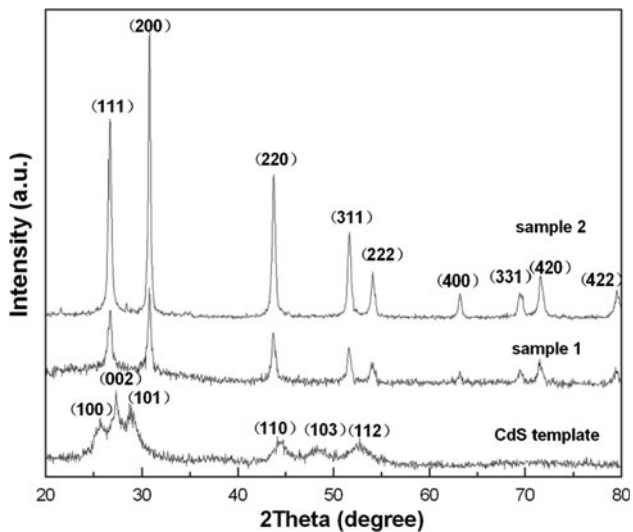


Fig. 1 XRD patterns of as-prepared CdS template, sample 1 and sample 2

image, the surface of these CdS solid spheres is rough, which confirms these spheres are aggregated from tiny primary crystals. As shown in Fig. 2c and d, after reacted in 30 °C for 14 h, hollow PbS spheres were formed. The majority of these as-obtained hollow spheres remain intact after centrifugation. Several broken spheres disclose the hollow interior of the product, which are highlighted with black arrows in the FESEM image. The average diameter of sample is measured to be about 285 nm (calculated from 100 particles from Fig. 2c). The corresponding TEM image confirms the product consists of well defined hollow

structures with narrow size distribution. Meanwhile, the shell thickness is measured to be about 90 nm. Moreover, Fig. 2d also reveals the polycrystalline nature of the hollow spheres which are comprised of numerous primary crystals with diameter about 13 nm (calculated from the corresponding XRD pattern). Figure 2e and f show the morphology of sample 2. The as-prepared PbS hollow spheres are also of high yield and with intact structures. Meanwhile, the shell thickness is thinner than that of sample 1. Therefore, the electron beam could penetrate the shell and disclose the hollow nature of this sample. Moreover, the outer diameter of the hollow spheres is about 320 nm (calculated from 100 particles in Fig. 2e) which experiences obvious growth compared with the diameter of CdS template. The TEM image suggests the interior of the product is completely hollowed and the shell is made of primary particles with diameter around 21 nm (from the Scherrer' equation) which is greater than that of sample 1. On the contrary, the shell thickness is measured to be about 60 nm which is smaller than that value of sample 1.

In order to disclose the growth mechanism of this conversion, time-dependent experiments were performed. For sample 1, different intermediate samples were collected at 1, 2, and 6 h. The corresponding XRD characterizations of these samples are displayed in Fig. 3a. For sample 2, the intermediate samples were collected at 5, 15, and 45 min and the XRD patterns are displayed in Fig. 3b. When the reaction time is 1 h (Fig. 3a), several weak diffraction peaks belonging to PbS could be observed (highlighted with asterisk markers), indicating a thin layer PbS was formed along the template. If the reaction time is further

Fig. 2 FESEM and TEM images of **a**, **b** CdS template; **c**, **d** sample 1; and **e**, **f** sample 2

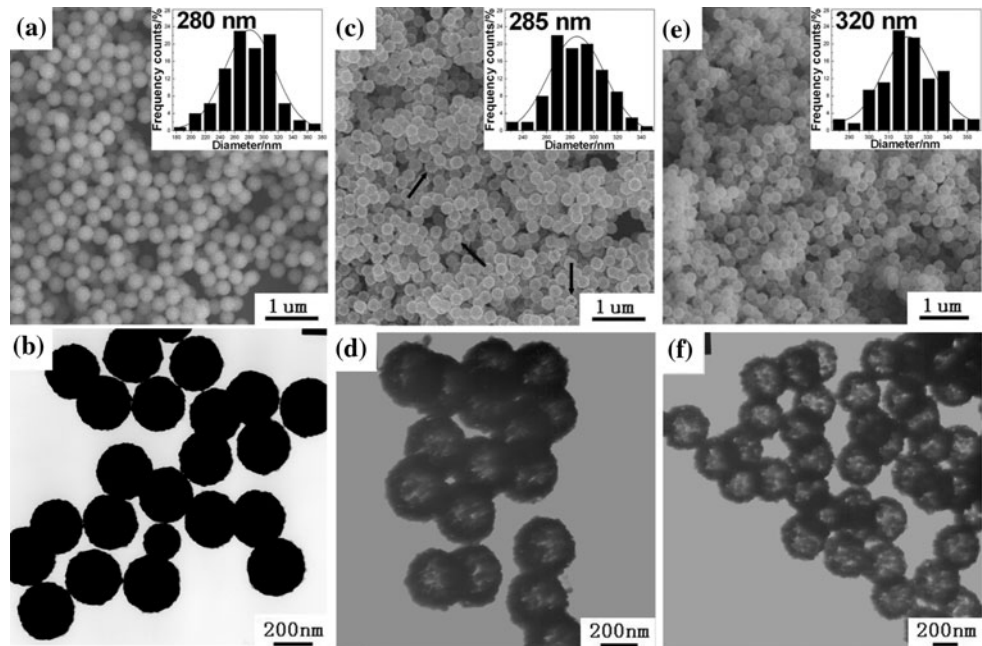
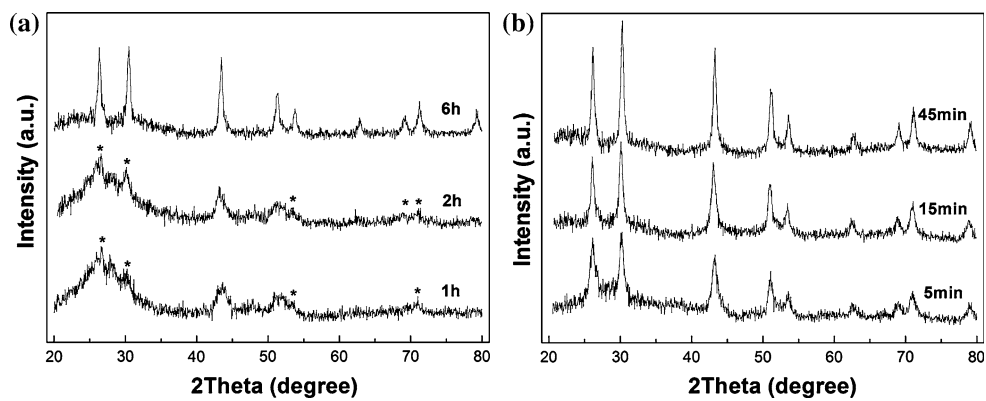


Fig. 3 XRD of the intermediate samples **a** sample 1 and **b** sample 2



prolonged to 2 h, the PbS peaks become stronger suggesting the proportion of PbS is elevated in this sample. When the reaction time finally reaches 6 h, the diffraction peaks belonging to CdS are too weak to be detected in the XRD curve. On the other hand, for sample 2, different intermediate samples collected at 5, 15, and 45 min were also characterized with XRD. Different from the conversion process of sample 1, almost at the very early stage, the CdS template was completely converted into pure PbS (Fig. 3b). It is interesting to find that, during this process, the width of the diffraction peaks becomes smaller indicating the growth of the primary particle of each sample. Based on Scherrer's equation, the particle size could be calculated to 9, 11, 15, and 21 nm for the each sample, respectively, collected at 5, 15, 45 min, and 2 h.

TEM was also adopted to monitor the growth process of these two samples. For sample 1, after 1 h, inconspicuous cavities appear between the core and shell which are highlighted with white arrows in Fig. 4a. It indicates a layer of PbS was coated on the surface of template and the thickness is measured to be around 50 nm. When the reaction is prolonged to 2 h, the cavity becomes greater to form a yolk-shell CdS/PbS structure (Fig. 4b) and the shell thickness is still about 50 nm. Further increasing the reaction to 6 h, the yolk is shrinking and the shell thickness grows to 70 nm (Fig. 4c). When the reaction time increases to 14 h, the yolk is completely removed to form the PbS hollow spheres and the final shell thickness is measured to be 90 nm. It is interesting to find that outer diameter of sample 1 is barely changed compared with that of the template (280–285 nm). For sample 2, after 5 min, the sample is still solid spheres (Fig. 4d), and these solid spheres are cubic PbS crystals which could be confirmed by the XRD characterization. When the reaction is carried out at 90 °C for 15 min, a cavity appears in the center of the solid spheres to form hollow sphere with shell thickness about 120 nm (Fig. 4e). When the reaction reaches to 45 min, the shell thickness becomes thinner (around

80 nm) (Fig. 4f). If the reaction is further prolonged to 2 h, the shell thickness finally decreases to about 60 nm. In the time-dependent experiments, the reaction was also elevated to 3 h, the shell became too thin to support itself and only broken spheres were yield. During this process, the shell thickness gradually reduces from 120 to 60 nm. On the other hand, the size of the particles comprised in the shell experiences a growth from 9 to 21 nm (from the XRD characterization).

In order to elucidate the growth mechanism, an illustration of these two processes was displayed in Fig. 4 g. When the CdS template was immersed into 0.3 M $\text{Pb}(\text{NO}_3)_2$ solution and the reaction was carried out under 30 °C, the diffusion of Pb^{2+} is mild and a layer of PbS firstly formed on the surface of the template. Because of lower solubility of PbS, the Pb^{2+} could substitute Cd^{2+} to form PbS crystals. During this process, S^{2-} ions generated from the dissolving of CdS is apt to diffuse out of the shell. On the contrary, the Pb^{2+} cations are diffusing from outside in. Moreover, compared with abundant Pb^{2+} , the amount of S^{2-} is rather smaller. Thus, in order to achieve the supersaturation for nucleation, the S^{2-} ions have to meet with high concentration Pb^{2+} . In the diffusion, the Pb^{2+} cations which have smaller radius transfer with higher rate than that of the S^{2-} . Therefore, the critical supersaturation was reached inside the formed PbS shell. Under this condition, the nucleation of PbS prefers to occur on the inner surface of the shell, which leads to an inward growth of the shell (Fig. 5a). Thus, although the shell thickness becomes greater gradually (from 50 to 90 nm), the outer diameter of the hollow sphere almost remains unchanged (285 nm). During this conversion, the shell growth is at the cost of the inner template. Therefore, the core could be finally removed from the hollow spheres without using core removing reagent. Considering the nucleation of PbS and the inwards growth of the shell largely depend on the different diffusion velocities between Pb^{2+} and S^{2-} ions, this conversion is defined as a kinetic-controlled process (KCP).

Fig. 4 TEM images of the intermediate samples collected at **a** 1 h, **b** 2 h, **c** 6 h for sample 1, and **d** 5 min, **e** 15 min, **f** 45 min for sample 2, **g** illustration of the growth processes

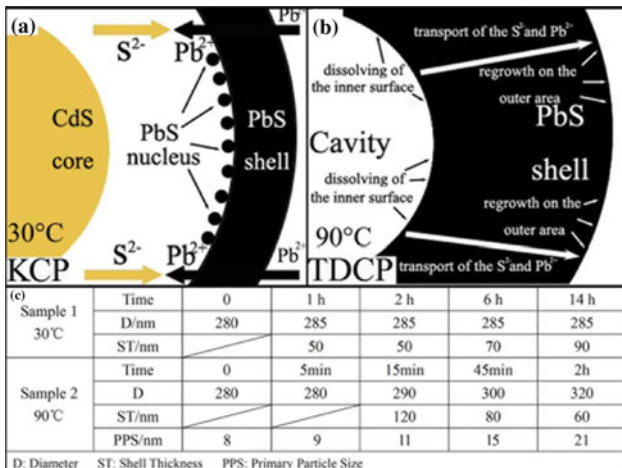
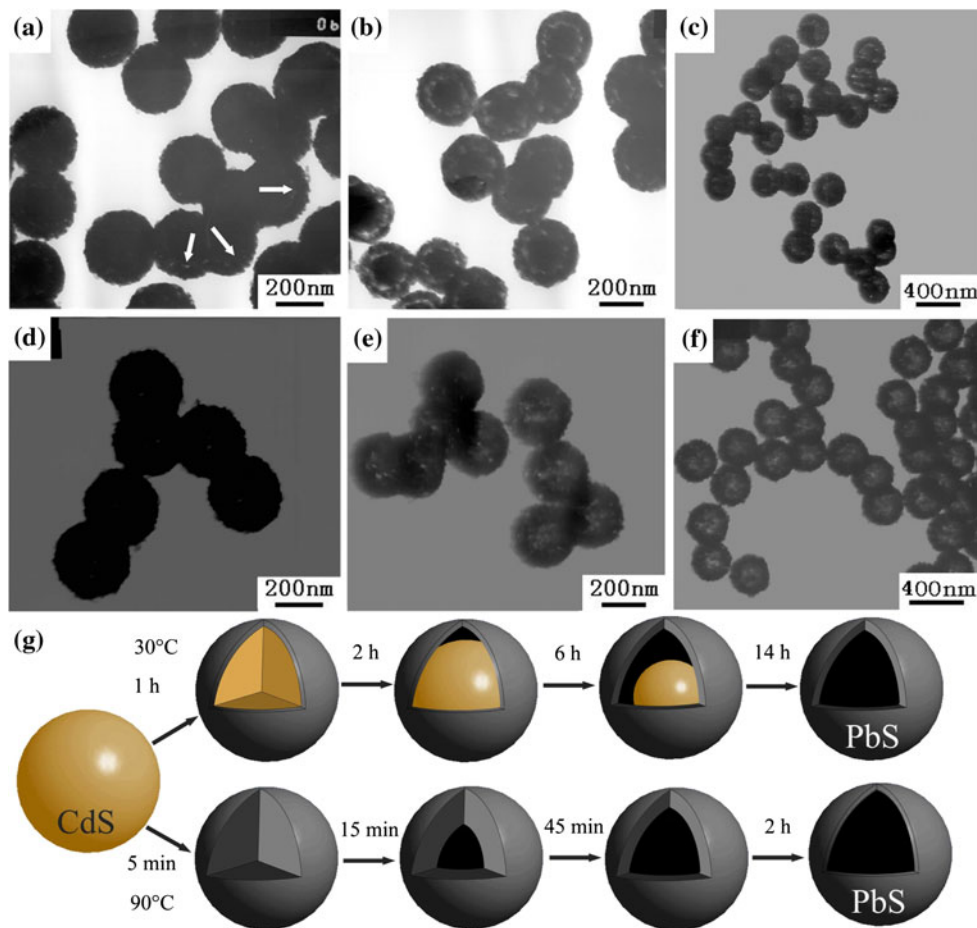


Fig. 5 Scheme of the growth mechanisms **a** KCP and **b** TDCP. **c** Detail changes of the structures collected at different time intervals

On the other hand, when the reaction temperature was elevated to 90 °C, the diffusion of the Pb²⁺ becomes so turbulence that the template could be radically converted into PbS after 5 min. According to Zeng's work [29], for an aggregate sphere, the primary particles located in the center

area have greater surface energy. Thus these particles are easily dissolved and diffuse out of the aggregate sphere. Afterwards, the as-formed Pb²⁺ and S²⁻ ions nucleate again and leads to the growth of the primary particles located on the surface area of the sphere (Fig. 5b). Therefore, for this conversion, the growth of outer particles (from 9 to 21 nm) is achieved by consuming the inner PbS primary particles. The hollowing of the solid PbS sphere started in the center area and the shell thickness become thinner and thinner in this conversion (from 120 to 60 nm). On the contrary, the diameter as-prepared PbS hollow spheres experienced an obvious growth compared with the staring template (from 280 to 320 nm). Time-dependent experiments confirm this conversion carried out at 90 °C mainly depends on the thermal stability of the primary particles consisted in the firstly formed PbS aggregate spheres, thus it is defined as a thermodynamic-controlled process (TDCP). Detailed variation of the outer diameter, shell thickness and primary particles sizes of the template, sample 1 and sample 2 are displayed in Fig. 5c.

The photoluminescence performances of these products were also investigated. Figure 6a and b depict the PL spectra of intermediate samples of sample 1. A strong peak

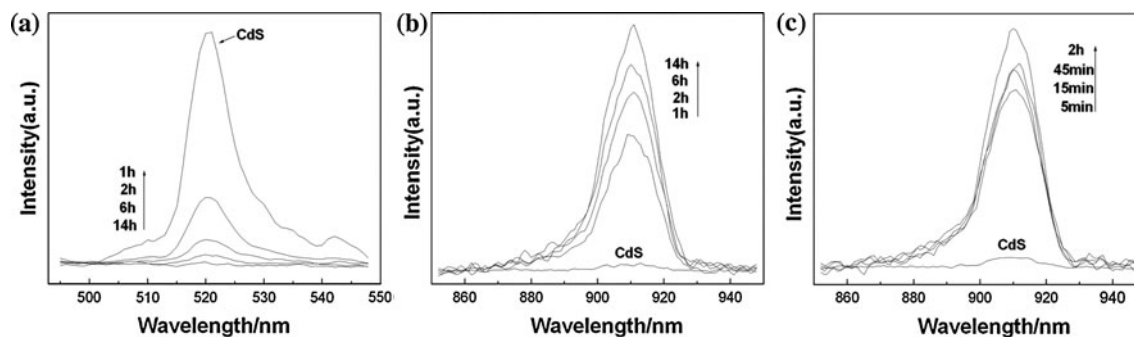


Fig. 6 PL spectra of as-prepared samples **a**, **b** prepared at 30 °C, **c** prepared at 90 °C

centered at 521 nm (2.38 eV) could be observed, which derives from the band edge recombination (2.4 eV) of CdS [31, 32]. The intensities of this peak decrease as increasing the reaction time, which indicates the CdS sample is gradually removed. In the red emission area, a peak centered at 911 nm could be detected which is attributed to the direct exciton recombination of the PbS crystal [33]. The increase of peak intensity reflects the proportion of PbS becomes greater with longer reaction time. After the CdS core was completely dissolved, the pure PbS hollow spheres exhibit the strongest emission peak among these samples. Figure 6c displays the PL spectra for the intermediates samples of sample 2. The characteristic PbS band edge emission centered at 911 nm could also be observed. It is obvious that the PbS hollow spheres with thin shell thickness possess better PL performance than the solid spheres and the hollow sphere with thicker shell. Therefore, these PbS hollow spheres could be possibly utilized to fabricate luminescent devices with emitting wavelengths between 800 and 1000 nm [34].

Conclusions

In summary, a facile method was developed to prepare PbS hollow spheres using CdS aggregate spheres as template. The growth processes from CdS solid to PbS hollow spheres were intensively studied. It was found the reaction temperature played a crucial role in manipulating the conversion process. When carried out at 30 °C, a gentle conversion defined as dynamics-controlled process was observed. Meanwhile, a thermodynamics-controlled mechanism was proposed for the radical conversion when the reaction was performed at 90 °C. According to their excellent photoluminescence performances, these as-prepared PbS hollow spheres could be considered as a promising material utilized in luminescent devices. Furthermore, this approach shows a high versatility for structural engineering of various targeted morphological products: core-shell structure, yolk-shell structure, and hollow structure.

Acknowledgements This work was supported by the National Natural Science Foundation of China (20571025) and Henan Innovation Project for University Prominent Research Talents (2005KYCX005).

References

- Zhu ZF, He ZL, Li JQ, Zhou JQ, Wei N, Liu DG (2010) *J Mater Sci*. doi:[10.1007/s10853-010-4837-1](https://doi.org/10.1007/s10853-010-4837-1)
- Kim SW, Kim M, Lee WY, Hyeon T (2002) *J Am Chem Soc* 124:7642
- He LF, Jia Y, Meng FL, Li MQ, Liu JH (2009) *J Mater Sci* 44:4326. doi:[10.1007/s10853-009-3645-y](https://doi.org/10.1007/s10853-009-3645-y)
- Wong MS, Cha JN, Choi KS, Deming TJ, Stucky GD (2002) *Nano Lett* 2:583
- Wang XX, Ji HF, Zhang X, Zhang H, Yang XL (2010) *J Mater Sci* 45:3981. doi:[10.1007/s10853-010-4470-z](https://doi.org/10.1007/s10853-010-4470-z)
- Fowler CE, Khushalani D, Mann S (2001) *Chem Commun* 1:2028
- Zhong Z, Yin Y, Gates B, Xia Y (2000) *Adv Mater* 12:206
- Hu JS, Guo YG, Liang HP, Wan LJ, Bai CL, Wang YG (2004) *J Phys Chem B* 108:9734
- Choi KH, Chae WS, Jung JS, Kim YR (2009) *Bull Korean Chem Soc* 30:1118
- Yan CL, Xue DF (2006) *J Phys Chem B* 110:25850
- Zhu YF, Fan DH, Shen WZ (2008) *Langmuir* 24:11131
- Wu DP, Jiang Y, Liu JJ, Yuan YF, Wu JS, Jiang K, Xue DF (2010) *Nanoscale Res Lett* 5:1779
- Gao JN, Li QS, Zhao HB, Li LS, Liu CL, Gong QH, Qi LM (2008) *Chem Mater* 20:6263
- Zhu HT, Wang JX, Wu DX (2009) *Inorg Chem* 48:7099
- Jiao SH, Xu LF, Jiang K, Xu DS (2006) *Adv Mater* 18:1174
- Liu J, Liu F, Gao K, Wu JS, Xue DF (2009) *J Mater Chem* 19:6073
- Wu DP, Xiao B, Liu N, Xiao Y, Jiang K (2010) *Mater Sci Eng B* 175:195
- Salavati-Niasari M, Loghman-Estarki MR, Davar F (2009) *Inorg Chim Acta* 362:3677
- Zhang ZH, Lee SH, Vittal JJ, Chin WS (2006) *J Phys Chem B* 110:6649
- Zhao XS, Xu SY, Liang LY, Li T, Cauchi S (2007) *J Mater Sci* 42:4265. doi:[10.1007/s10853-006-0679-2](https://doi.org/10.1007/s10853-006-0679-2)
- Zhao N, Oseidach TP, Bulovic MV et al (2010) *ACS Nano* 4:3743
- Li F, Qin QH, Wu JF, Li Z (2010) *J Mater Sci* 45:348. doi:[10.1007/s10853-009-3942-5](https://doi.org/10.1007/s10853-009-3942-5)
- Zhu JJ, Liu SW, Palchik O, Koltypin Y, Gedanken A (2000) *J Solid State Chem* 153:342
- Zhao NN, Qi LM (2006) *Adv Mater* 18:359

25. Salavati-Niasari M, Sobhani A, Davar F (2010) J Alloy Compd 507:77
26. Hu Y, Chen JF, Jin XZ, Chen WM (2005) Mater Lett 59:234
27. Wang SF, Gu F, Lv MK (2006) Langmuir 22:398
28. Yan CL, Zou LJ, Xue DF, Xu JS, Liu MN (2008) J Mater Sci 43:2263. doi:[10.1007/s10853-007-2072-1](https://doi.org/10.1007/s10853-007-2072-1)
29. Yang HG, Zeng HC (2004) J Phys Chem B 108:3492
30. Li XH, Li JX, Li GD, Liu DP, Chen JS (2007) Chem Eur J 13:8754
31. Ge JP, Li YD (2004) Adv Funct Mater 14:157
32. Cortes A, Svasand E, Lavayen V, Segura R, Haberle P (2010) J Mater Sci 45:4958. doi:[10.1007/s10853-010-4350-6](https://doi.org/10.1007/s10853-010-4350-6)
33. Warner JH, Thomsen E, Watt AR, Heckenberg NR, Rubinsztein-Dunlop H (2005) Nanotechnology 16:175
34. Warner JH, Watt AR, Thomsen E, Heckenberg N, Meredith P, Rubinsztein-Dunlop H (2005) J Phys Chem B 109:9001